(4-Aminopyridine)–PLGA–PEG as a Novel Thermosensitive and Locally Injectable Treatment for Acute Peripheral Nerve Injury

Kristen M. Manto, **Prem Kumar Govindappa**

Department of Orthopaedics and Rehabilitation, Center for Orthopaedic Research and Translational Science, The Pennsylvania State University College of Medicine, Milton S. Hershey Medical Center, Hershey, Pennsylvania 17033, United States

Daniele Parisi

Department of Materials Science and Engineering, The Pennsylvania State University, University Park, Pennsylvania 16802, United States

Zara Karuman, **Brandon Martinazzi**, **John P. Hegarty**, **M A Hassan Talukder**, **John C. Elfar**

Department of Orthopaedics and Rehabilitation, Center for Orthopaedic Research and Translational Science, The Pennsylvania State University College of Medicine, Milton S. Hershey Medical Center, Hershey, Pennsylvania 17033, United States

Abstract

Traumatic peripheral nerve injury (TPNI) represents a major medical problem that results in loss of motor and sensory function, and in severe cases, limb paralysis and amputation. To date, there are no effective treatments beyond surgery in selective cases. In repurposing studies, we found that daily systemic administration of the FDA-approved drug 4-aminopyridine (4-AP) enhanced functional recovery after acute peripheral nerve injury. This study was aimed at constructing a novel local delivery system of 4-AP using thermogelling polymers. We optimized a thermosensitive (4-AP)–poly(lactide-*co*-glycolide)–*b*-poly(ethylene glycol)–*b*-poly(lactide-*co*-glycolide) (PLGA–PEG–PLGA) block copolymer formulation. (4-AP)–PLGA–PEG exhibited controlled release of 4-AP both *in vitro* and *in vivo* for approximately 3 weeks, with clinically relevant safe serum levels in animals. Rheological investigation showed that (4-AP)–PLGA–PEG underwent a solution to gel transition at 32 °C, a physiologically relevant temperature, allowing us to administer it to an injured limb while subsequently forming an *in situ* gel. A single local administration of (4-AP)–PLGA–PEG remarkably enhanced motor and sensory functional recovery on post-sciatic nerve crush injury days 1, 3, 7, 14, and 21. Moreover, immunohistochemical studies of injured nerves treated with (4-AP)-PLGA-PEG demonstrated an increased expression of neurofilament heavy chain (NF-H) and myelin protein zero (MPZ)

proteins, two major markers of nerve regeneration. These findings demonstrate that (4-AP)–PLGA–PEG may be a promising long-acting local therapeutic agent in TPNI, for which no pharmacologic treatment exists.

Graphical Abstract
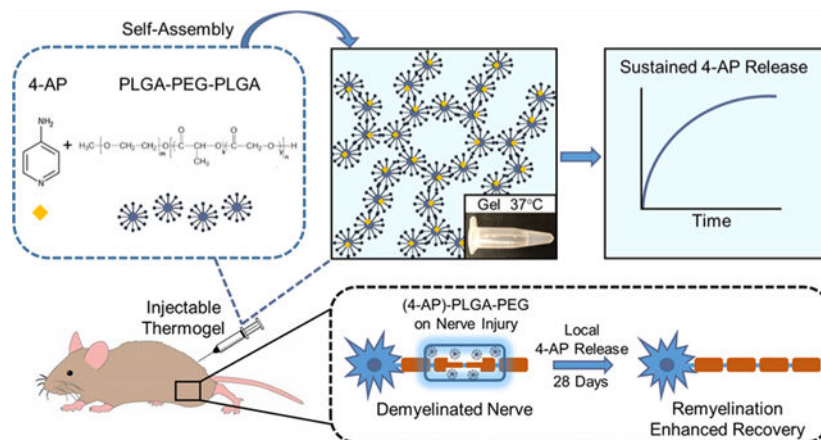
Keywords

peripheral nerve; sciatic nerve; crush injury; traumatic nerve injury; thermogel; block copolymer; 4-aminopyridine; PLGA; PEG

INTRODUCTION

Traumatic peripheral nerve injury (TPNI) is a major health problem occurring in approximately 3% of all trauma patients.[1–3] Most TPNIs result from either acute blunt trauma, crush, or compression. TPNI can lead to significant loss of function with disability, which can be permanent or transient depending on the extent of axonal injury. Neuropraxic lesions which retain axonal continuity and have segmental loss of the myelin sheath can recover spontaneously. On the other hand, recovery of transected nerves depends on prompt surgical intervention.[4–6] Surgical management of these injuries is challenging since performing surgery too early can harm the potential for spontaneous recovery, while delaying surgery can miss the time window necessary to intervene.[7–9] In addition, although nerve conduits are materials which can aid in surgical nerve repair, they provide mainly mechanical support alone.[10] There is no standard of care for crush injuries, the most prevalent TPNI. Thus, there is an unmet need for a pharmacologic agent which can enhance functional recovery after TPNI.

In repurposing studies, systemic 4-aminopyridine (4-AP) has been shown to enhance functional recovery after traumatic nerve injury in mice by improving sciatic function index (SFI) and nerve conduction velocity.[11] 4-AP is a nonspecific antagonist of voltage-gated potassium (K_v) channels.[12] It is approved by the United States Food and Drug Administration (FDA) for neurodegenerative disorders such as multiple sclerosis, where it restores impaired impulse propagation and improves walking performance. Demyelination

of the peripheral nerve exposes outwardly rectifying K_v channels, causing loss of potassium ions and impairment in nerve conduction. Due to the higher density of K_v channels in internodia than at nodes of Ranvier, 4-AP blockage of potassium channels restores and prolongs action potentials with increased amplitude in demyelinated axons.[13]

Despite its efficacy, use of systemic 4-AP may garner safety concerns due to unpredictable blood levels, with high doses causing seizures. More common side effects include sleep disturbance, nausea, vertigo, and headache. Thus, a local controlled-release formulation could help mitigate these effects by directly targeting a nerve injury site with improved efficacy at lower dosages.[14] Local delivery of 4-AP is also desirable to improve patient compliance through a single local injection instead of daily oral dosing. In addition, repurposing an FDA-approved drug could greatly hasten the translation of our findings into clinical practice. Based on preliminary data on systemic 4-AP, we sought to develop a controlled-release formulation which could be locally injected near a nerve injury site and deliver drug for several weeks.

Recently, block copolymers have emerged as novel biodegradable, thermosensitive drug delivery systems for controlled release of incorporated small molecules.[15–17] Application of these delivery systems would be especially relevant in orthopaedic practice where injury sites are easily identifiable and can be locally targeted. We hypothesized that 4-AP could interact with amphiphilic polyethylene glycol/polylactic acid-*co*-glycolic acid (PEG/PLGA), both FDA-approved, biodegradable, and biocompatible polymers, to promote the release of 4-AP at a controlled rate. To test this hypothesis, we synthesized a PLGA/PEG triblock copolymer containing 4-AP (Figure 1) and examined its physiochemical and thermogelling properties. Secondary structure of block copolymer aqueous solutions was examined for the *in vitro* release profile of 4-AP. Finally, *in vivo* drug release and efficacy of our optimized 4-AP thermogel were determined. In this study for the first time, we investigated the effects of a novel long-acting local 4-AP thermogel for the treatment of acute peripheral nerve injury. We demonstrate that (4-AP)–PLGA–PEG enhances the speed and extent of functional recovery and promotes remyelination in acutely damaged peripheral nerves.

MATERIALS AND METHODS

Animals.

Male C57BL/6J mice (10 weeks old; Jackson Laboratories, Bar Harbor, Maine) weighing 25 ± 3 g were used in this study. Experimental design and animal protocols were approved by the Institutional Animal Care and Use Committee (IACUC) at The Pennsylvania State University College of Medicine.

Block Copolymer Synthesis and Characterization.

Poly-(lactide-*co*-glycolide)–*b*-poly(ethylene glycol)–*b*-poly(lactide-*co*-glycolide) (1700–1500–1700 Da, LA/GA 15:1, 94%:6% LA/GA, PolySciTech) and 4-aminopyridine (4-AP, Sigma-Aldrich) were used without further purification. 4-AP was incorporated in PLGA–PEG–PLGA triblock copolymer solution (1× PBS, pH 7.4, polymer concentration: 20 wt %), stirred at 4 °C until it was completely dissolved, and characterized using proton nuclear

magnetic resonance (^{1}H NMR) to confirm the composition. Experiments using ^{1}H NMR were carried out with Bruker Avance II 600 MHz instrument equipped with a TCI cryo-probe. Standard presaturation pulse programs from the Bruker pulse sequence library were used to suppress residual D_2O solvent. The samples were prepared at room temperature and experiments were performed at 25°C.

Rheological Characterization of Block Copolymer Aqueous Solutions.

Small amplitude oscillatory shear experiments were performed in a Discovery Hybrid Rheometer (DHR-3) from TA Instruments (New Castle, DE, USA). The rheometer was equipped with a 60 mm diameter stainless steel cone with a truncation gap of 28 μm and 1° cone angle. The cone was installed in the upper portion of the rheometer, which also hosted the motor and transducer for both torque and normal forces. The bottom plate was constituted by a Peltier element used to control the temperature with an accuracy of ±0.1 °C.

A typical volume of 1.2 mL of solution was poured onto the bottom plate at 20 °C to minimize evaporation. The loading was followed by a trimming stage, where the excess sample was removed before leading the cone to the measuring gap (μm). Once in the measuring position, the solution was surrounded by an organic noninteracting oil to avoid water evaporation. The viscosity of the oil was much lower than that of the aqueous solution so that the torque signal was largely unaffected by the presence of the oil. Rapid experiments with no oil at room temperature corroborated the results obtained with oil. Experiments conformed to previous work.[18]

The linear viscoelastic limits were probed by means of shear strain amplitude sweep experiments at 10 rad/s and at the temperature of interest. The range of temperatures explored was 10–40 °C. A shear strain of 0.03 strain units ensured the linear viscoelastic regime for the whole temperature window. Temperature sweep tests were all performed at 10 rad/s and 0.03 strain units, from 10 to 40 °C with a heating rate of 0.5 °C/min. The instrument accounted for thermal expansion of the measuring systems and the resulting change of gap, which served to ensure a constant measuring gap regardless of the temperature used in the experiment. The time evolution of the shear response of solutions was monitored in time sweep experiments where the frequency remained 10 rad/s and the shear strain remained 0.03 strain units. Frequency sweep experiments were performed at 0.03 strain units, well within the linear viscoelastic regime, at 25 °C and in the range of frequencies 100–0.1 rad/s.

The monitored rheological functions were: storage modulus G' (elastic contribution to the material response), loss modulus G'' (viscous contribution to the material response), and ratio G''/G', or the loss factor $\tan(\delta)$, with δ being the phase shift between the sinusoidal input exerted by the instrument and the material response output. $\tan(\delta)$ was used as a parameter to detect gelation.

In Vitro 4-AP Release from PLGA–PEG–PLGA Hydrogels.

Polymer solutions containing varying concentrations of 4-AP (2, 5, 10 μg/μL) were transferred to 1.5 mL test tubes and the samples were incubated in a water bath at 37 °C to convert them to physical hydrogels. Next, PBS (1×, pH 7.4) was added to each test tube as

release media and the samples were left in the water bath at 37 °C for 30 days. At designated time points, release media was extracted from the tubes and replaced with the same amount of fresh PBS to maintain the sink condition. The amount of 4-AP released into the media was measured with UV–Vis spectrophotometry (Thermo Scientific NanoDrop One Spectrophotometer) to determine cumulative drug release over time, as in related work.[19] Quantification of amount of drug released was done using a 4-AP standard curve generated using known concentrations of the drug.

In Vivo Degradation of Thermogel and 4-AP Release in Mice.

Mice ($n = 9$) were given (4-AP)–PLGA–PEG at a body-weight-adjusted dose of 1.4 mg/kg using thermogel with a 4-AP concentration of 2 μg/μL. Blood was retro-orbitally collected at various time points to sample serum via centrifugation. Serum 4-AP concentration was determined using high-performance liquid chromatography (HPLC) to ensure that the serum levels in mice remained within the human tolerable limit of 100 ng/mL.[20] Circulating levels of 4-AP in mouse serum samples were determined using ABSciex 4000 Q Trap mass spectrometry (MS) coupled with a Waters Acquity ultraperformance liquid chromatography separation system (UPLC/MS/MS) in the Mass Spectrometry Core Facility. 4-AP-d_4 was used as an internal standard. The multiple reaction monitoring mode was used to analyze and quantify 4-AP and 4-AP-d_4, with the transitions of m/z 95 > 78 for 4-AP and 99 > 82 for 4-AP-d_4. Quantification of 4-AP used a standard curve constructed by plotting the ratio of the peak area of 4-AP to the peak area of 4-AP-d_4 against 4-AP concentration (0.01–20 μM). All peaks were integrated and quantified by ABSciex Multiquan 2.1 software (Framingham, MA).

To assess *in vivo* biodegradation of (4-AP)–PLGA–PEG, mice were anesthetized with intraperitoneal (IP) ketamine (100 mg/kg)/xylazine (10 mg/kg). The sciatic nerves were surgically exposed at weekly time points to observe location, adherence to the nerve, and mass of the gel.

Mouse Model of Sciatic Nerve Crush Injury.

Sciatic nerve crush injury was performed as previously described with pressure-gauge-tethered forceps.[21] Briefly, after IP ketamine (100 mg/kg)/xylazine (10 mg/kg) anesthesia, the right hindlimb was shaved and prepared with alcohol swabs and povidone–iodine (Betadine). Under a binocular microscope (Model PZMIII, World Precision Instruments), a lateral skin incision (~2.5 cm) was made along the length of the femur and the sciatic nerve (SN) was bluntly exposed through the iliotibial band. Crush injury was performed ~3 mm proximal to the SN trifurcation using calibrated forceps (3.3 mm tip width; 18–1107, Miltex Instruments, York, PA) for a 30 s duration at a pressure of 4.4 MPa. Skin was closed via surgical staples and post-operative slow release buprenorphine (0.05 mg/kg) was given subcutaneously as an analgesic. The experimental animals ($n = 5$/group) were randomly assigned to Sham (normal saline, 0.1 mL/mouse, IP), SN crush injury with saline (normal saline, 0.1 mL/mouse, IP), SN crush injury with systemic 4-AP (4-AP, 2 mg/kg, IP), SN crush injury with PLGA–PEG vehicle (PLGA–PEG, ~20 μL on sciatic nerve injury site), and SN crush injury with (4-AP)–PLGA–PEG ((4-AP)–PLGA–PEG, 1.4 mg/kg, ~20 μL on sciatic nerve injury site) groups. Systemic 4-AP was given IP once daily for 28 days. Local

administration groups received (4-AP)–PLGA–PEG immediately after crush injury. Post-injury functional recovery was assessed by walking track analysis (WTA), sensory nerve testing (SNT), and grip strength testing on days 1, 3, 7, 14, 21, and 28. The animals were euthanized on post-injury day 28 to harvest sciatic nerves for histological analysis.

Sciatic Function Index (SFI).

To evaluate *in vivo* global motor functional recovery, sciatic function index (SFI) was determined by WTA as previously described.[21] Briefly, mice were trained to walk freely along a 77 by 7 cm corridor lined with paper and individual footprints of the hindlimbs were obtained before surgery as a baseline and on post-surgery days 1, 3, 7, 14, 21, and 28. At least three measurable footprints for each hindlimb were obtained. Two blinded observers measured three footprints per hindlimb with digital calipers. SFI was calculated using three parameters: (1) toe spread (TS, first to the fifth toe), (2) total print length (PL), and (3) intermediate toe spread (IT, second to the fourth toe) and the following formula: SFI = $-38.3\{(EPL - NPL)/NPL\} + 109.5\{(ETS - NTS)/NTS\} + 13.3\{(EIT - NIT)/NIT\} - 8.8$, where E is for experimental (injured) and N is for normal (contralateral uninjured) sides.

Hindlimb Grip Strength Test.

A grip strength meter (BIO-GS3, Bioseb-In Vivo Research Instruments, Pinellas Park, FL) was used to measure hindlimb grip strength.[22] Briefly, the mice were restrained by holding the scruff and base of the tail. Mice were allowed to hold the grid and were gently pulled along the length of the sensor grid until the grip was released. The force value was recorded five times per animal to calculate the average grip strength. Attention was paid to minimize paw injury and habit formation during each trial.

Von Frey Test.

Mice were placed in a transparent polycarbonate chamber ($\sim 10 \times 10$ cm) with a metallic mesh floor approximately 25 cm above the bench. Animals were acclimatized prior to testing. SNT was performed as previously described using a von Frey filament unit (NC12775-08, Touch Test Sensory Evaluators).[23–25] Briefly, the filament pressure (1 g force) was applied to the plantar surface of the hindlimb through the mesh floor and the animal withdrawing its paw was considered a positive response. The withdrawal reflex of the hindlimb was recorded five times per animal to calculate the average percent response.

Sciatic Nerve Processing and Immunohistochemical Analysis.

Sciatic nerve processing and immunohistochemical staining were performed as previously described with slight modification.[25] SNs were harvested on post-injury day 28 from the ipsilateral hindlimbs of mice. Nerves were fixed in 4% paraformaldehyde (PFA) solution overnight, washed with 70% alcohol, and embedded in paraffin. A microtome (Model RM2235, Leica, Buffalo Grove, IL) was used to cut serial 5 μm transverse sections from the paraffin blocks. Tissue sections were deparaffinized and serially rehydrated with xylene and ethanol and antigen retrieval was performed using 10 mM sodium citrate buffer (pH 6.0). Permeabilization and nonspecific binding blocking were done using 1% Triton X-100 and 5% goat serum, respectively. Primary antibody staining was performed with anti-NF-H

(1:1000; NB300-135, Novus Biologicals) and anti-MPZ (1:1000; PZ0, Aves Laboratories) followed by secondary antibody incubation with Alexa Fluor 488 (1:1000; A11008, Invitrogen) and Alexa Fluor 647 (1:1000; A21449, Invitrogen). Staining without primary antibodies served as a control for nonspecific fluorescence. Nuclei were counterstained with ProLong Gold antifade reagent with DAPI (P36935; Invitrogen) and sections were observed under a fluorescent microscope (ZEISS Apotome 2). Stained nerve tissues were analyzed and immunofluorescence intensity was quantified using ImageJ software (National Institutes of Health, Bethesda, MD).

Feasibility of Local (4-AP)–PLGA–PEG Injection under Ultrasound Guidance.

To verify if (4-AP)–PLGA–PEG could be locally and noninvasively administered to a targeted nerve injury site, ultrasound guidance was used for local (4-AP)–PLGA–PEG injection. Briefly, mice ($n = 5$) were anesthetized with 5% isoflurane in an induction chamber and fur over their hindlimb was shaved using an animal clipper. Skin was prepped in an aseptic fashion and the mice were placed on the mouse-handling stage in a prone position. A Vevo 3100 (Visual Sonics, Canada) microultrasound machine with a 40 MHz probe was used to image longitudinal sections of the proximal hindlimb. The probe was manually used to scan the hindlimb proximally and distally to ensure identification of the sciatic nerve. A 20 G needle was manually inserted into the hindlimb to first confirm its presence and was then positioned over the sciatic nerve. A 20 μL volume of (4-AP)–PLGA–PEG was then injected onto the sciatic nerve. Following injection, the sciatic nerve was surgically exposed to confirm correct anatomic placement and adherence of the gel on the nerve.

Statistical Analysis.

All the results were expressed as mean ± standard error of the mean (SEM). For group comparison, the statistical differences of mean values were analyzed by least significant difference (LSD) t tests as well as one-way and two-way analysis of variance (ANOVA). A p value of less than 0.05 was considered as significant.

RESULTS

Block Copolymer Synthesis and Characterization.

As shown in Figure 2, the NMR spectra of 4-AP are ^{1}H NMR (D$_2$O): δ8.02 (d, $J = 5.4$ Hz), 6.69 (d, $J = 5.4$ Hz). The spectra of PLGA–PEG are ^{1}H NMR (D$_2$O): 3.68 (s), 1.60–1.50 (m),1.46–1.38 (m), 1.31 (d, $J = 7.0$ Hz). After mixing of 4-AP with PLGA–PEG at room temperature, the ^{1}H NMR (D$_2$O): δ7.94 (d, $J = 6.4$ Hz), 6.83 (d, $J = 6.4$ Hz), 3.68 (s), 1.46–1.38 (m), 1.29 (dd, $J = 6.8$ Hz, 0.8 Hz). The spectra revealed that the chemical shifts of the mixture showed a significant change corresponding to both aromatic protons of 4-AP from δ8.02 to 7.94 and δ6.69 to 6.83, respectively. In addition, the PLGA–PEG aliphatic region was changed from δ1.31 to 1.29 after mixing. These findings of chemical shift changes indicate that the chemical environment changes for 4-AP when mixed with PLGA–PEG.

Rheological Characterization of Block Copolymer Aqueous Solutions.

Both PLGA–PEG–PLGA and PLGA–PEG–PLGA polymers with 4-AP were soluble in PBS at room temperature and underwent solution-to-gel (sol–gel) transitions with increasing temperature. Figure 3A shows the changes in modulus of PLGA–PEG–PLGA and PLGA–PEG–PLGA polymers with varying concentrations of 4-AP as a function of temperature. At low or room temperature, the loss modulus G'' was greater than the storage modulus G', reflecting a solution-free-flowing phase. An abrupt increase in modulus was observed along with the formation of physical hydrogels as the temperature increased. The sol–gel transition temperatures (T_{gel}), the crossover point of G'' and G', of PLGA–PEG and 2 μg/μL (4-AP)–PLGA–PEG, the concentration used in animals, were 31.3 and 32 °C, respectively (Figure 3A). T_{gel} increased with increasing 4-AP concentration (Figure 3A). However, despite the moduli being shifted as concentration increased, all concentrations exhibited gelation, and the gel windows of the polymers covered body temperature, indicating that the thermogels were suitable for biomedical applications. To further support this, as shown in Figure 3B, the loss factor tan(δ) was less than 1 for the thermogels at temperatures at or above 32 °C, indicating solid-like behavior and gel formation at physiologically relevant temperatures. 4-AP (10 μg/μL) formed a weak gel as indicated by the limited temperature range in which tan(δ) was less than 1. The solution displayed a second crossover point from solid to liquid behavior, while the other concentrations remained solid at temperatures above 32 °C.

Figure 3C,D shows the change in moduli as a function of time. As observed in Figure 3C, the sol–gel transition for 2 μg/μL PLGA–PEG, the concentration used in animals, occurred in 19 s. Persistence of solid-like behavior was observed after gelation occurred, demonstrated by the plateau of moduli over time, indicating a strong physical gel. We next studied the reversibility of gelation in Figure 3D and found that the sol–gel transition was fully reversible and occurred in 1228 s. This suggests that if 4-AP gel is placed in an incorrect location, it can be cooled to a liquid and moved elsewhere.

In Vitro 4-AP Release from PLGA–PEG–PLGA Hydrogels.

We evaluated the *in vitro* release profiles of 4-AP from PLGA–PEG–PLGA at varying concentrations (2, 5, 10 μg/μL) to determine if the thermogel could release clinically relevant doses of 4-AP at a controlled rate. The data in Figure 4 show the cumulative amounts of 4-AP released over 28 days. The loaded 4-AP on the μg level exhibited a burst release within the first day followed by a sustained release at a controlled rate up to 28 days for all loaded 4-AP amounts. Specifically, *in vitro* release of 4-AP from PLGA–PEG hydrogels exhibited an overall burst biphasic profile.[26] Moreover, cumulative release was proportional to total loaded amount of 4-AP. The average cumulative release amount by day 28 was 69, 78, and 43% for 10, 5, and 2 μg/μL, respectively.

In Vivo Degradation of Thermogel and 4-AP Release in Mice.

Since the initial burst release in drug delivery systems can pose a safety concern if the drug concentration reaches beyond the toxicity threshold, we ensured that 4-AP serum levels after thermogel administration were safe even at peak release.[26] Serum levels of 4-AP peaked 1 h after administration and never exceeded the human tolerable limit of 100 ng/mL known to cause adverse side effects in humans (Figure 5A). Serum 4-AP levels were nearly

undetectable after 21 days of administration (Figure 5B), indicating that (4-AP)–PLGA–PEG releases systemically detectable amounts of 4-AP at a sustained rate for approximately 21 days *in vivo*.

To determine whether the gel was correctly administered to the sciatic nerve, we exposed the mouse hindlimb to observe the gel location, adherence, and integrity after administration. As shown in Figure 6, (4-AP)–PLGA–PEG turned opaque when administered to the nerve, indicating thermogelation. The gel remained directly on the sciatic nerve injury site for over 21 days, although its overall mass decreased due to controlled polymeric degradation. Taken together with *in vivo* release data, (4-AP)–PLGA–PEG likely releases 4-AP locally for over 21 days, since the polymer is still present on the injury site at this time.

(4-AP)–PLGA–PEG Effect on Peripheral Nerve Functional Recovery.

In previous studies, we have shown that systemic 4-AP administration improves motor functional recovery after sciatic nerve crush injury.[11] The effects of a novel locally applicable 4-AP thermogel on sciatic nerve crush injury and on motor and sensory outcomes post-injury required functional evaluation. We found (4-AP)–PLGA–PEG improved post-injury functional recovery (SFI) on days 1 (−70.7 vs −89.7), 3 (−55.3 vs −77.7), 7 (−42.2 vs −79.0), and 14 (−7.8 vs −39.3) compared to saline control (Figure 7A, $*p < 0.05$). (4-AP)–PLGA–PEG outperformed systemic treatment at the highest daily dose as well as vehicle control.

(4-AP)–PLGA–PEG improved grip strength on post-injury days 3 (38.51 vs 25.49 kg), 7 (36.96 vs 24.66 kg), 14 (42.67 vs 29.52 kg), 21 (56.15 vs 28.51 kg), and 28 (62.71 vs 54.56 kg) compared to saline control (Figure 7B, $*p < 0.05$). Grip strength was also significantly improved compared to 4-AP systemic and vehicle treatments (Figure 7B). Since grip strength examines neuromuscular function, this suggests that (4-AP)–PLGA–PEG treatment improves volitional muscle strength in proportion to improved global motor function as indicated by SFI following crush injury.[27]

To assess the effect of (4-AP)–PLGA–PEG on sensory nerve recovery, we performed von Frey filament testing. Von Frey filament testing provides a noninvasive assessment of sensory function and cutaneous sensation by studying paw withdrawal thresholds.[28] Similar to motor functional results, (4-AP)–PLGA–PEG treatment significantly improved the withdrawal reflex (percent response to filament) as compared to the saline group (Figure 7C,$*p < 0.05$) on post-injury days 1 (13.33 vs 0%), 3 (36 vs 12%), 7 (68 vs 44%), 14 (100 vs 44%), and 21 (100 vs 88%). (4-AP)–PLGA–PEG also outperformed systemic and vehicle treatments. These findings demonstrate that (4-AP)–PLGA–PEG can improve sensory nerve function after crush injury.

Immunohistochemical Analysis of (4-AP)–PLGA–PEG Effect on Peripheral Nerve Remyelination.

One of the main properties known to contribute to impulse conduction in nerves is myelination.[29–31] Following peripheral nerve injury, axonal demyelination coupled with subsequent remyelination over time has been shown to correlate with injury severity.[32] In addition, the degree of axonal remyelination directly correlates to the degree of functional

recovery post-injury.[32] To determine the effect of 4-AP thermogel on nerve remyelination, transverse sectioned nerves were stained for neurofilament-H (NF-H), a structural component of large myelinated axons, and myelin protein zero (MPZ), the most abundant protein in myelin, using immunohistochemistry.[33,34] Significant increases in myelin were observed by immunofluorescence for both NF-H and MPZ in (4-AP)–PLGA–PEG-treated nerves compared to saline-treated nerves on post-injury day 28 (Figure 8B,C, $*p < 0.05$). (4-AP)–PLGA–PEG-treated nerves contained approximately 2.5-fold more MPZ and 7.3-fold more NF-H protein in the lesion area than nerves from saline- and vehicle-treated animals. Although systemic 4-AP treatment significantly increased NF-H and MPZ fluorescence intensities compared to saline, (4-AP)–PLGA–PEG significantly surpassed this effect.

Feasibility of Local (4-AP)–PLGA–PEG Injection under Ultrasound Guidance.

Ultrasound-guided injections are commonly performed not only in orthopaedics but across all fields of medicine. We tested whether our thermogel could be locally and noninvasively administered to a nerve injury site using this common imaging modality. Under ultrasound guidance, we were able to clearly visualize the mouse sciatic nerve (Figure 9A) and needle (Figure 9B). We visualized the positioning of the needle directly around the nerve injury site to inject (4-AP)–PLGA–PEG (Figure 9C). After injection, based on its relative density to local tissue, (4-AP)–PLGA–PEG could be clearly observed on the sciatic nerve (Figure 9D), demonstrating the formulation's clinical utility.

DISCUSSION

This study was undertaken to determine the applicability of a novel locally injectable 4-AP delivery system, its material and pharmacokinetic characteristics, and its effects on neuromuscular functional recovery following sciatic nerve crush injury in mice. Here, we report for the first time that 4-AP can be used as a thermosensitive local therapeutic agent that promotes motor and sensory functional recovery of the limb with better preservation of axonal myelination.

Peripheral nerve injury is a substantial clinical problem which lacks satisfactory treatment options beyond surgery in selected cases. The current treatment of choice for nerve laceration is microsurgical repair.[35] However, there is no standard of care for crush injuries, which are more numerous and for which full recovery is not guaranteed. Surgery, which is reserved for settings of complete nerve laceration, is optimally performed early since delayed repair can be detrimental to motor and sensory recovery.[36,37] Nerve conduits can sometimes assist in surgical repair of lacerations but are ill-suited for the more common crush injuries.[38] An injectable gel, if effective, would be an optimal nonsurgical intervention for the most common type of peripheral nerve injury clinically encountered. A polymer-based treatment could also offer a physical guide for axonal regeneration like conduits do, with the additional benefits of localized controlled drug release and ease of application.[39]

Our earlier studies demonstrated the efficacy of daily systemic 4-AP administration in improving functional recovery after traumatic peripheral nerve injury.[11,40,41] However, adverse systemic side effects and potential barriers to patient compliance could make systemic administration suboptimal. In addition, in nerve injuries where lesions are easily

identifiable, a locally injectable pharmacologic agent would be ideal to directly target a nerve injury, minimizing side effects, improving efficacy, and limiting the frequency of drug administration. Recently, we have shown that transdermal formulation of 4-AP can promote functional recovery of the limb with better preservation of axonal myelin sheath thickness and improved nerve conduction after sciatic nerve crush injury.[42] In this study, we found that a novel thermosensitive and locally injectable formulation of 4-AP enhanced both the speed and extent of recovery of motor and sensory function after TPNI, analyzed by SFI, grip strength, and von Frey measurements. Local treatment at a dose well below the systemic dose resulted in reproducible, clinically relevant improvements in global motor and sensory functional recovery after sciatic nerve injury. The neuroprotective effect of (4-AP)–PLGA–PEG was also evident in immunohistochemical evaluation of injured peripheral nerves. Our findings demonstrated significant increases in two major markers of peripheral nerve regeneration, NF-H and MPZ, in the late stage of nerve recovery, suggesting its role as a potential myeloprotective and regenerative agent. These findings are consistent with our previous studies on the effects of systemic 4-AP in traumatic nerve injury.[11]

In vitro release studies of (4-AP)–PLGA–PEG showed that the formulation could sustainably release 4-AP for up to 1 month after administration. Pharmacokinetic studies showed 4-AP serum levels were nearly undetectable by day 21, at total doses to the injury site far below the systemically tolerable level. Taken together, we believe (4-AP)–PLGA–PEG releases 4-AP at systemically detectable levels for approximately 3 weeks, after which the remaining local drug is too low to be detected systemically.

Rheological investigation demonstrated that our delivery system undergoes a liquid to solid phase transition at temperatures only slightly lower than human body temperature and that, once formed, the gel remains as a strong matrix over time. Thus, (4-AP)–PLGA–PEG can be used as an injectable at room temperature, after which it will spontaneously form a gel around a suspected nerve injury site for controlled-release of 4-AP. We found 10 μg/μL to be the limiting 4-AP concentration in PLGA–PEG, since this concentration exhibited a solid to liquid crossover point at increasing temperature. This is likely due to hydrolysis of PLGA by the amino group of 4-AP which hinders gelation at increasing concentrations. Because we desired a strong gel which would persist over time within a wide temperature window *in vivo*, we chose to use the 2 μg/μL thermogel in all animal experiments. We also examined the reversibility of gelation for circumstances when the thermogel may potentially be misplaced in the body. The reversibility of sol–gel transition suggests that if the gel is placed in an incorrect location, it can easily be cooled to a liquid.

Since the solution to gel transition of our formulation occurs within a physiologically relevant temperature window, we sought to prove that we could successfully noninvasively inject it under ultrasound guidance, a common imaging modality. In humans, ultrasound-guided injections have been explored extensively and injections of agents including steroids are routinely performed.[43–47] Even in the small mouse hindlimb, we were able to visualize the sciatic nerve and successfully inject 4-AP thermogel onto the injury site. It remains to be seen whether ultrasound-guided injection of our agent in humans is feasible. However, there are reasons to believe that the larger structures in humans and currently available ultrasound guidance systems in clinical practice would allow trials without surgical exposure. The

feasibility of noninvasive 4-AP thermogel injection could be very significant in patients for several reasons. First, it could reduce or eliminate the need for surgical exposure in cases where the nerve is not lacerated or for patients who are not surgical candidates. Second, it would allow for repeated administration of the agent in the outpatient setting or in settings with limited surgical resources. Thus, the feasibility of ultrasound-guided injection offers great promise for the translation of (4-AP)–PLGA–PEG into clinical practice.

FDA-approved 4-AP has been utilized for decades to improve nerve conduction in various neurodegenerative disorders such as multiple sclerosis and myasthenia gravis.[48,49] In these disorders, the efficacy of 4-AP is thought to be immediate and attributable to its effects of improving impulse propagation in demyelinated axons. Our results support this idea in which a nerve crush injury with predominantly myelin-based dysfunction functionally improved after (4-AP)–PLGA–PEG administration, suggesting improved nerve conduction. However, long-term, more sustained 4-AP effects may contribute to the observed results. Published studies have linked electrical stimulation in peripheral nerve injury to improvements in axonal remyelination and reinnervation.[50–53] We tested these effects by assessing functional parameters and myelination markers after 4-AP had been implanted. The continued functional improvement and remyelination 28 days post-injury observed are likely not solely attributable to the short-term axonal effects of 4-AP.

Despite the interesting findings with (4-AP)–PLGA–PEG administration, our study has some limitations. First, we did not quantify myelinated axon counts, axon diameter, or myelin thickness. Second, we did not perform electrophysiological examination of the injured nerve before and after (4-AP)–PLGA–PEG treatment or study related muscle characteristics, although we have published the short-term effects of 4-AP thermogel on muscle tension recovery in rat and effects of 4-AP on electrodiagnostics.[11,54] Third, we did not investigate the molecular and cellular mechanism(s) of 4-AP thermogel-induced improvement of nerve morphology and function. Finally, we studied the more common crush injury and not the permanent denervation model.[55]

In summary, this study was particularly designed to determine the feasibility of (4-AP)–PLGA–PEG administration and its usefulness in traumatic peripheral nerve injury. *In vitro* characterization demonstrated that our formulation releases 4-AP at a sustained rate for several weeks and undergoes liquid to solid phase transition at body temperature, offering promise as a long-acting injectable therapeutic. Consistent with pharmacologic trials and our studies with systemic and transdermal 4-AP administrations, we observed that the serum concentration after local (4-AP)–PLGA–PEG administration was dose-dependent and the maximal peak serum concentration was reached at 60 min.[41,42,56–58] Functional and histological findings demonstrated that 4-AP thermogel is effective in TPNI with significant positive effects on both motor and sensory functional recovery and nerve remyelination. Future studies in nerve crush and transection models will be important to demonstrate the electrophysiological outcomes as well as underlying mechanisms of (4-AP)–PLGA–PEG in TPNI recovery with injury severity. Our findings may have significant clinical implications because this formulation can be used to provide sustained local drug delivery directly at the injury site, without the need for daily oral dosing and associated need for patient compliance.[59,60]

CONCLUSIONS

In conclusion, we provide preclinical evidence that (4-AP)–PLGA–PEG has the potential to be a promising alternative to systemic 4-AP to treat patients with peripheral nerve injury. Our thermosensitive, controlled-release formulation consists of two FDA-approved, biodegradable, and biocompatible hydrogels encapsulating an already FDA-approved small molecule. The translation of this therapeutic for use in regenerating acutely damaged peripheral nerves could be rapid, and efforts should be made to consider its utility. Therefore, this study provides the rationale for further investigations to determine the important mechanistic insights in local 4-AP-induced neuromuscular protection in the setting of peripheral neuro-trauma with continuity where no medical treatment is currently available.

ACKNOWLEDGMENTS

ABBREVIATIONS

TPNI	traumatic peripheral nerve injury
4-AP	4-amino-pyridine
PEG	polyethylene glycol
PLGA	polylactic acid-*co*-glycolic acid
^{1}H NMR	proton nuclear magnetic resonance
IP	intraperitoneal
SN	sciatic nerve
SFI	sciatic function index
WTA	walking track analysis
SNT	sensory nerve test
NF-H	neurofilament-H
MPZ	myelin protein zero

REFERENCES

(1). Taylor CA; Braza D; Rice JB; Dillingham T The incidence of peripheral nerve injury in extremity trauma. Am. J. Phys. Med. Rehabil 2008, 87, 381–385. [PubMed: 18334923]

(2). Sakuma M; Minev IR; Gribi S; Singh B; Woolf CJ; Lacour SP Chronic electrical nerve stimulation as a therapeutic intervention for peripheral nerve repair. Bioelectron Med 2015, 2, 43–48.

(3). Asplund M; Nilsson M; Jacobsson A; von Holst H Incidence of traumatic peripheral nerve injuries and amputations in Sweden between 1998 and 2006. Neuroepidemiology 2009, 32, 217–228. [PubMed: 19174611]

(4). Campbell WW Evaluation and management of peripheral nerve injury. Clin. Neurophysiol 2008, 119, 1951–1965. [PubMed: 18482862]

(5). Niver GE; Ilyas AM Management of radial nerve palsy following fractures of the humerus. Orthop. Clin. North Am 2013, 44, 419–424. [PubMed: 23827843]

(6). Ljungquist KL; Martineau P; Allan C Radial nerve injuries. J. Hand Surg 2015, 40, 166–172.

(7). Shah A; Jebson PJ Current treatment of radial nerve palsy following fracture of the humeral shaft. J. Hand Surg 2008, 33, 1433–1434.

(8). Birch R; Misra P; Stewart MP; Eardley WG; Ramasamy A; Brown K; Shenoy R; Anand P; Clasper J; Dunn R; et al. Nerve injuries sustained during warfare: part I-Epidemiology. J. Bone Jt. Surg., Br Vol. 2012, 94-B, 523–528.

(9). Bishop J; Ring D Management of radial nerve palsy associated with humeral shaft fracture: a decision analysis model. J. Hand Surgery 2009, 34, 991–996.

(10). Rebowe R; Rogers A; Yang X; Kundu SC; Smith TL; Li Z Nerve Repair with Nerve Conduits: Problems, Solutions, and Future Directions. J. Hand Microsurg 2018, 10, 61–65. [PubMed: 30154617]

(11). Tseng KC; Li H; Clark A; Sundem L; Zuscik M; Noble M; Elfar J 4-Aminopyridine promotes functional recovery and remyelination in acute peripheral nerve injury. EMBO Mol. Med 2016, 8, 1409–1420. [PubMed: 27861125]

(12). Leussink VI; Montalban X; Hartung HP Restoring Axonal Function with 4-Aminopyridine: Clinical Efficacy in Multiple Sclerosis and Beyond. CNS Drugs 2018, 32, 637–651. [PubMed: 29992409]

(13). Bostock H; Sears TA; Sherratt RM The effects of 4-aminopyridine and tetraethylammonium ions on normal and demyelinated mammalian nerve fibres. J. Physiol 1981, 313, 301–15. [PubMed: 7277221]

(14). Hauser SL; Johnston SC 4-Aminopyridine: new life for an old drug. Ann. Neurol 2010, 68, A8–A9.

(15). Youxin L; Kissel T Synthesis and properties of biodegradable ABA triblock copolymers consisting of poly(L-lactic acid) or poly(L-lactic-co-glycolic acid) A-blocks attached to central poly(oxyethylene) B-blocks. J. Controlled Release 1993, 27, 247–257.

(16). Hadjichristidis N; Iatrou H; Pitsikalis M; Mays J Macromolecular architectures by living and controlled/living polymerizations. Prog. Polym. Sci 2006, 31, 1068–1132.

(17). Ding J; Zhang J; Li J; Li D; Xiao C; Xiao H; Yang H; Zhuang X; Chen X Electrospun polymer biomaterials. Prog. Polym. Sci 2019, 90, 1–34.

(18). Chen Q; Wang Y; Lu Z; Feng Y Thermoviscosifying polymer used for enhanced oil recovery: rheological behaviors and core flooding test. Polym. Bull 2013, 70, 391–401.

(19). Parameswaran-Thankam A; Parnell CM; Watanabe F; RanguMagar AB; Chhetri BP; Szwedo PK; Biris AS; Ghosh A Guar-Based Injectable Thermoresponsive Hydrogel as a Scaffold for Bone Cell Growth and Controlled Drug Delivery. ACS omega 2018, 3, 15158–15167. [PubMed: 30555998]

(20). Sindhurakar A; Mishra AM; Gupta D; Iaci JF; Parry TJ; Carmel JB Clinically Relevant Levels of 4-Aminopyridine Strengthen Physiological Responses in Intact Motor Circuits in Rats, Especially After Pyramidal Tract Injury. Neurorehabilitation and neural repair 2017, 31, 387–396. [PubMed: 28107804]

(21). Elfar JC; Jacobson JA; Puzas JE; Rosier RN; Zuscik MJ Erythropoietin accelerates functional recovery after peripheral nerve injury. J. Bone Joint Surg. Am 2008, 90, 1644–1653. [PubMed: 18676893]

(22). Hwee DT; Kennedy A; Ryans J; Russell AJ; Jia Z; Hinken AC; Morgans DJ; Malik FI; Jasper JR Fast skeletal muscle troponin activator tirasemtiv increases muscle function and performance in the B6SJL-SOD1G93A ALS mouse model. PLoS One 2014, 9, e96921. [PubMed: 24805850]

(23). Bonin RP; Bories C; De Koninck Y A simplified up-down method (SUDO) for measuring mechanical nociception in rodents using von Frey filaments. Mol. Pain 2014, 10, 1744-8069-10-26.

(24). Zhao WJ; Gao ZY; Wei H; Nie HZ; Zhao Q; Zhou XJ; Wang YX Spinal Damino acid oxidase contributes to neuropathic pain in rats. J. Pharmacol. Exp. Ther 2010, 332, 248–254. [PubMed: 19828879]

(25). Govindappa PK; Talukder MAH; Gurjar AA; Hegarty JP; Elfar JC An effective erythropoietin dose regimen protects against severe nerve injury-induced pathophysiological changes with improved neural gene expression and enhances functional recovery. Int. Immunopharmacol 2020, 82, 106330. [PubMed: 32143001]

(26). Yoo J; Won YY Phenomenology of the Initial Burst Release of Drugs from PLGA Microparticles. ACS Biomater. Sci. Eng 2020, 6, 6053–6062. [PubMed: 33449671]

(27). Takeshita H; Yamamoto K; Nozato S; Inagaki T; Tsuchimochi H; Shirai M; Yamamoto R; Imaizumi Y; Hongyo K; Yokoyama S Modified forelimb grip strength test detects aging-associated physiological decline in skeletal muscle function in male mice. Sci. Rep 2017, 7, 42323. [PubMed: 28176863]

(28). Martinov T; Mack M; Sykes A; Chatterjea D Measuring changes in tactile sensitivity in the hind paw of mice using an electronic von Frey apparatus. J. Visualized Exp 2013, e51212.

(29). Sanders FK; Whitteridge D Conduction velocity and myelin thickness in regenerating nerve fibres. J. Physiol 1946, 105, 152–174.

(30). Waxman SG Determinants of conduction velocity in myelinated nerve fibers. Muscle Nerve 1980, 3, 141–150. [PubMed: 6245357]

(31). Ikeda M; Oka Y The relationship between nerve conduction velocity and fiber morphology during peripheral nerve regeneration. Brain Behav. 2012, 2, 382–390. [PubMed: 22950042]

(32). Hayes KC Fampridine-SR for multiple sclerosis and spinal cord injury. Expert Rev. Neurother 2007, 7, 453–61. [PubMed: 17492896]

(33). Garcia ML; Lobsiger CS; Shah SB; Deerinck TJ; Crum J; Young D; Ward CM; Crawford TO; Gotow T; Uchiyama Y; Ellisman MH; Calcutt NA; Cleveland DW NFM is an essential target for the myelin-directed "outside-in" signaling cascade that mediates radial axonal growth. J. Cell Biol 2003, 163, 1011–20. [PubMed: 14662745]

(34). Raasakka A; Ruskamo S; Kowal J; Han H; Baumann A; Myllykoski M; Fasano A; Rossano R; Riccio P; Burck J; et al. Molecular structure and function of myelin protein P0 in membrane stacking. Sci. Rep 2019, 9, 642. [PubMed: 30679613]

(35). Lien SC; Cederna PS; Kuzon WM Optimizing skeletal muscle rein-nervation with nerve transfer. Hand Clin. 2008, 24, 445–454. [PubMed: 18928892]

(36). Engel AG; Stonnington HH Trophic functions of the neuron. II. Denervation and regulation of muscle. Morphological effects of denervation of muscle. A quantitative ultrastructural study. Ann. N. Y. Acad. Sci 1974, 228, 68–88. [PubMed: 4526276]

(37). Gordon T; Tyreman N; Raji MA The basis for diminished functional recovery after delayed peripheral nerve repair. J. Neurosci 2011, 31, 5325–j5334. [PubMed: 21471367]

(38). Houshyar S; Bhattacharyya A; Shanks R Peripheral Nerve Conduit: Materials and Structures. ACS Chem. Neurosci 2019, 10, 3349–3365. [PubMed: 31273975]

(39). Zhang X; Qu W; Li D; Shi K; Li R; Han Y; Jin E; Ding J; Chen X Functional polymer-based nerve guide conduits to promote peripheral nerve regeneration. Adv. Mater. Interfaces 2020, 7, 2000225.

(40). Yue L; Talukder MA; Gurjar A; Lee JI; Noble M; Dirksen RT; Chakkalakal J; Elfar JC 4-Aminopyridine attenuates muscle atrophy after sciatic nerve crush injury in mice. Muscle Nerve 2019, 60, 192–201. [PubMed: 31093982]

(41). Hsu CG; Talukder MA; Yue L; Turpin LC; Noble M; Elfar JC Human equivalent dose of oral 4-aminopyridine differentiates nerve crush injury from transection injury and improves post-injury function in mice. Neural Regener. Res 2020, 15, 2098–107.

(42). Clark AR; Hsu CG; Hassan Talukder MA; Noble M; Elfar JC Transdermal delivery of 4-aminopyridine accelerates motor functional recovery and improves nerve morphology following sciatic nerve crush injury in mice. Neural Regener. Res 2020, 15, 136–144.

(43). Ehsanian R; Schneider BJ; Kennedy DJ; Koshkin E Ultrasound-guided cervical selective nerve root injections: a narrative review of literature. Reg. Anesth. Pain Med 2021, rapm-2020–102325.

(44). Ayekoloye CI; Nwangwu O Ultrasound-Guided Versus Anatomic Landmark-Guided Steroid Injection of the Subacromial Bursa in the Management of Subacromial Impingement: A Systematic Review of Randomised Control Studies. Indian J. Orthop 2020, 54, 10–19. [PubMed: 32952904]

(45). Wang D Image Guidance Technologies for Interventional Pain Procedures: Ultrasound, Fluoroscopy, and CT. Curr. Pain Headache Rep 2018, 22, 6. [PubMed: 29374352]

(46). Brose SW; Montfort J; Gustafson KJ; Mittebrun I; Gauriloff S; Mosher M; Bourbeau DJ Ultrasound-Guided Steroid Injection of the Pisotriquetral Joint: A Multidisciplinary Effort. Am. J. Phys. Med. Rehabil 2017, 96, 904–907. [PubMed: 28582272]

(47). Barile A; La Marra A; Arrigoni F; Mariani S; Zugaro L; Splendiani A; Di Cesare E; Reginelli A; Zappia M; Brunese L; Duka E; Carrafiello G; Masciocchi C Anaesthetics, steroids and platelet-rich plasma (PRP) in ultrasound-guided musculoskeletal procedures. Br. J. Radiol 2016, 89, 20150355. [PubMed: 27302491]

(48). Lundh H; Nilsson O; Rosen I Effects of 4-aminopyridine in myasthenia gravis. J. Neurol., Neurosurg. Psychiatry 1979, 42, 171–5. [PubMed: 422965]

(49). Hayes KC The use of 4-aminopyridine (fampridine) in demyelinating disorders. CNS Drug Rev 2004, 10, 295–316. [PubMed: 15592580]

(50). Gordon T; Brushart TM; Amirjani N; Chan KM The potential of electrical stimulation to promote functional recovery after peripheral nerve injury–comparisons between rats and humans. Acta. Neurochir. Suppl 2007, 100, 3–11. [PubMed: 17985535]

(51). Vivo M; Puigdemasa A; Casals L; Asensio E; Udina E; Navarro X Immediate electrical stimulation enhances regeneration and reinnervation and modulates spinal plastic changes after sciatic nerve injury and repair. Exp. Neurol 2008, 211, 180–93. [PubMed: 18316076]

(52). Wan L; Zhang S; Xia R; Ding W Short-term low-frequency electrical stimulation enhanced remyelination of injured peripheral nerves by inducing the promyelination effect of brain-derived neurotrophic factor on Schwann cell polarization. J. Neurosci. Res 2010, 88, 2578–2587. [PubMed: 20648648]

(53). Wake H; Lee PR; Fields RD Control of local protein synthesis and initial events in myelination by action potentials. Science 2011, 333, 1647–51. [PubMed: 21817014]

(54). Gurjar AA; Manto KM; Estrada JA; Kaufman M; Sun D; Talukder MAH; Elfar JC 4-Aminopyridine: A Single-Dose Diagnostic Agent to Differentiate Axonal Continuity in Nerve Injuries. Mil. Med 2021, 186, 479–485. [PubMed: 33499448]

(55). Kemp SWP; Cederna PS; Midha R Comparative outcome measures in peripheral regeneration studies. Exp. Neurol 2017, 287, 348–357. [PubMed: 27094121]

(56). Vollmer T; Blight AR; Henney HR Steady-state pharmacokinetics and tolerability of orally administered fampridine sustained-release 10-mg tablets in patients with multiple sclerosis: a 2-week, open-label, follow-up study. Clin. Ther 2009, 31, 2215–2223. [PubMed: 19922892]

(57). Davis FA; Stefoski D; Rush J Orally administered 4-aminopyridine improves clinical signs in multiple sclerosis. Ann. Neurol 1990, 27, 186–192. [PubMed: 2317014]

(58). Uges DRA; Sohn YJ; Greijdanus B; Scat AHJ; Agoston S 4-Aminopyridine kinetics. Clin. Pharmacol. Ther 1982, 31, 587–593. [PubMed: 7075108]

(59). Paudel KS; Milewski M; Swadley CL; Brogden NK; Ghosh P; Stinchcomb AL Challenges and opportunities in dermal/transdermal delivery. Ther. Delivery 2010, 1, 109–31.

(60). Prausnitz MR; Langer R Transdermal drug delivery. Nat. Biotechnol 2008, 26, 1261–1268. [PubMed: 18997767]
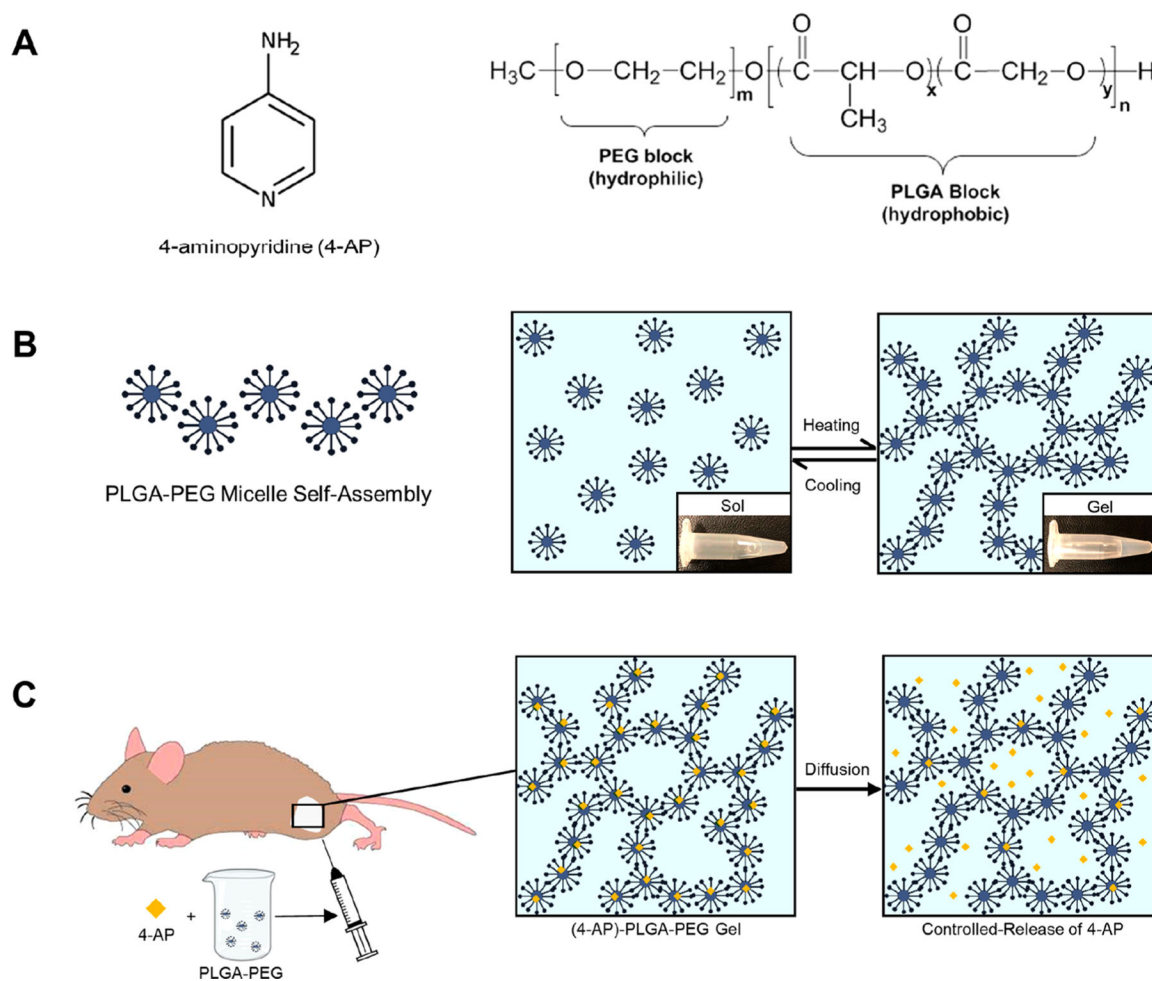
Figure 1.
Schematic representation of a (4-AP)-loaded thermogel as a local controlled-release delivery system. (A) Chemical structures of 4-AP and PLGA–PEG, respectively. (B) Amphiphilic polyester–PEG–polyester triblock copolymers self-assemble into micelles in aqueous solution at room temperature and form a solid gel via cross-links at higher temperature. (C) 4-AP can be incorporated into the triblock copolymer at room temperature and injected into an animal in liquid phase. Once the formulation reaches body temperature, it forms an *in situ* hydrogel for controlled release of 4-AP.
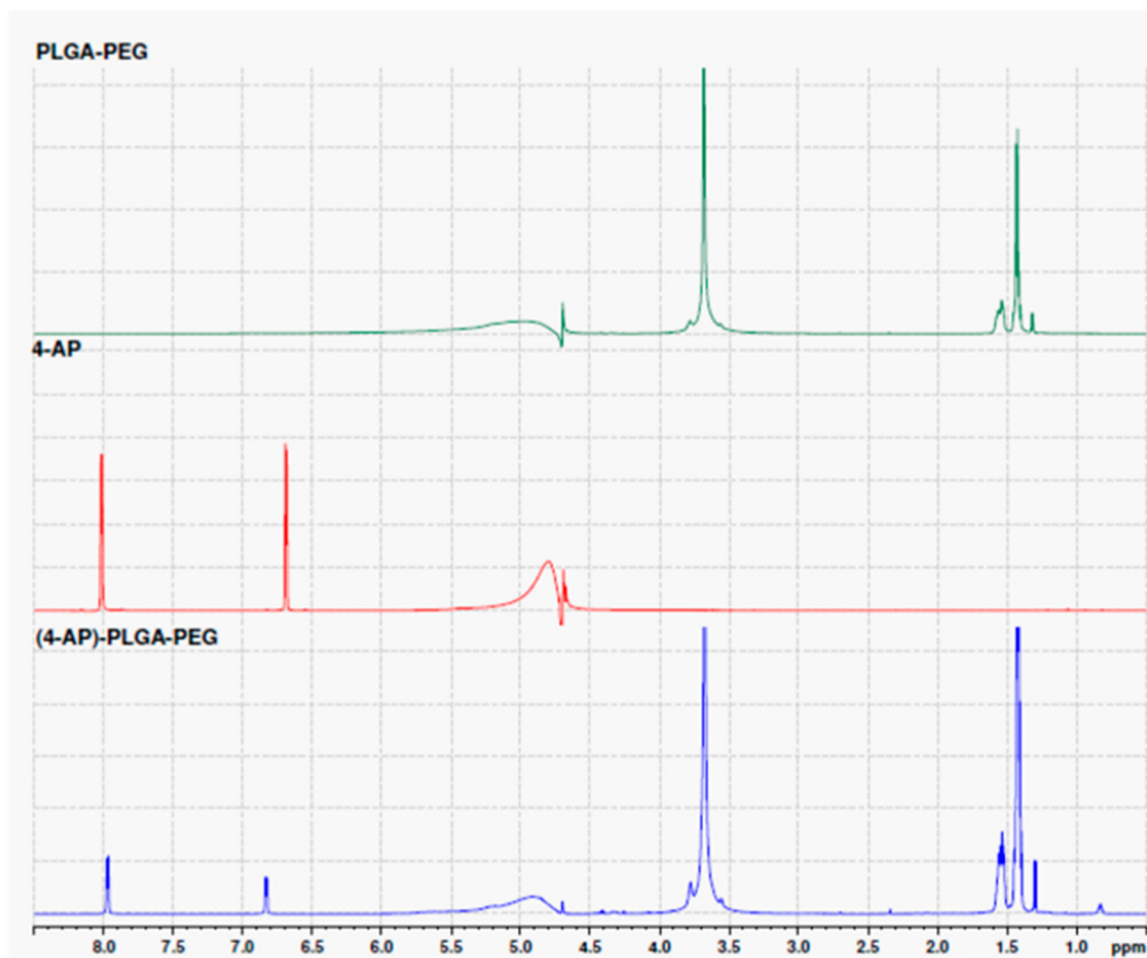
Figure 2.
^{1}H NMR spectra of PLGA–PEG, 4-AP, and (4-AP)–PLGA–PEG. The chemical shifts of the mixture showed significant change at both aromatic protons of 4-AP from δ8.02 to 7.94 and δ6.69 to 6.83, respectively, when mixed with PLGA–PEG. In addition, the PLGA–PEG aliphatic region was changed from δ1.31 to 1.29 after mixing.
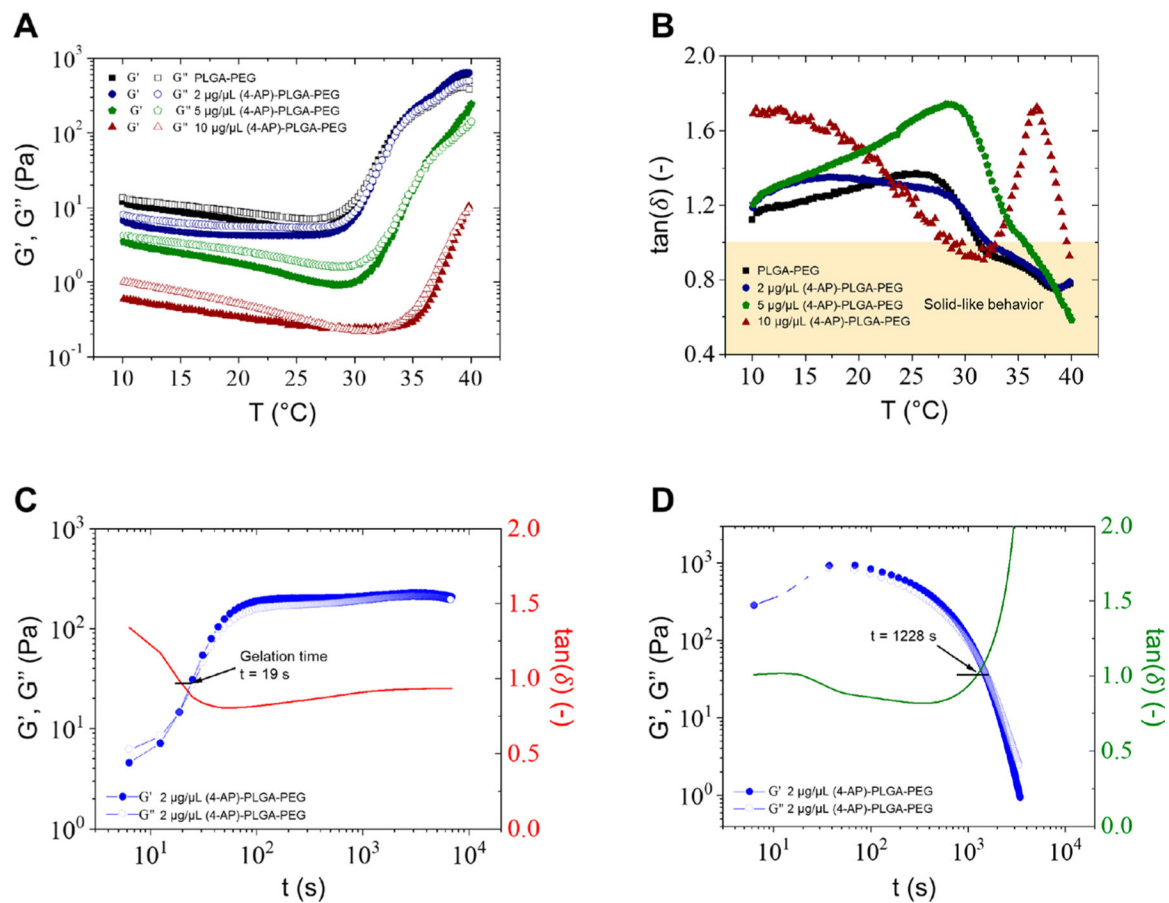
Figure 3.
Rheological investigation of copolymer aqueous solutions. (A) Gelation temperatures of PLGA–PEG and 2 μg/μL (4-AP)–PLGA–PEG were 31.3 and 32 °C, respectively. Gelation temperature increased with increasing 4-AP concentration. (B) Tan(δ) was less than 1, indicating solid-like behavior, for all concentrations at body temperature except 10 μg/μL, which exhibited a second solid to liquid crossover point at increasing temperature. (C) The solution to gel (sol–gel) transition of 2 μg/μL (4-AP)–PLGA–PEG occurred in 19 s and was followed by persistence of solid-like behavior over time. (D) The sol–gel transition of 2 μg/μL (4-AP)–PLGA–PEG was fully reversible and occurred in 1228 s.
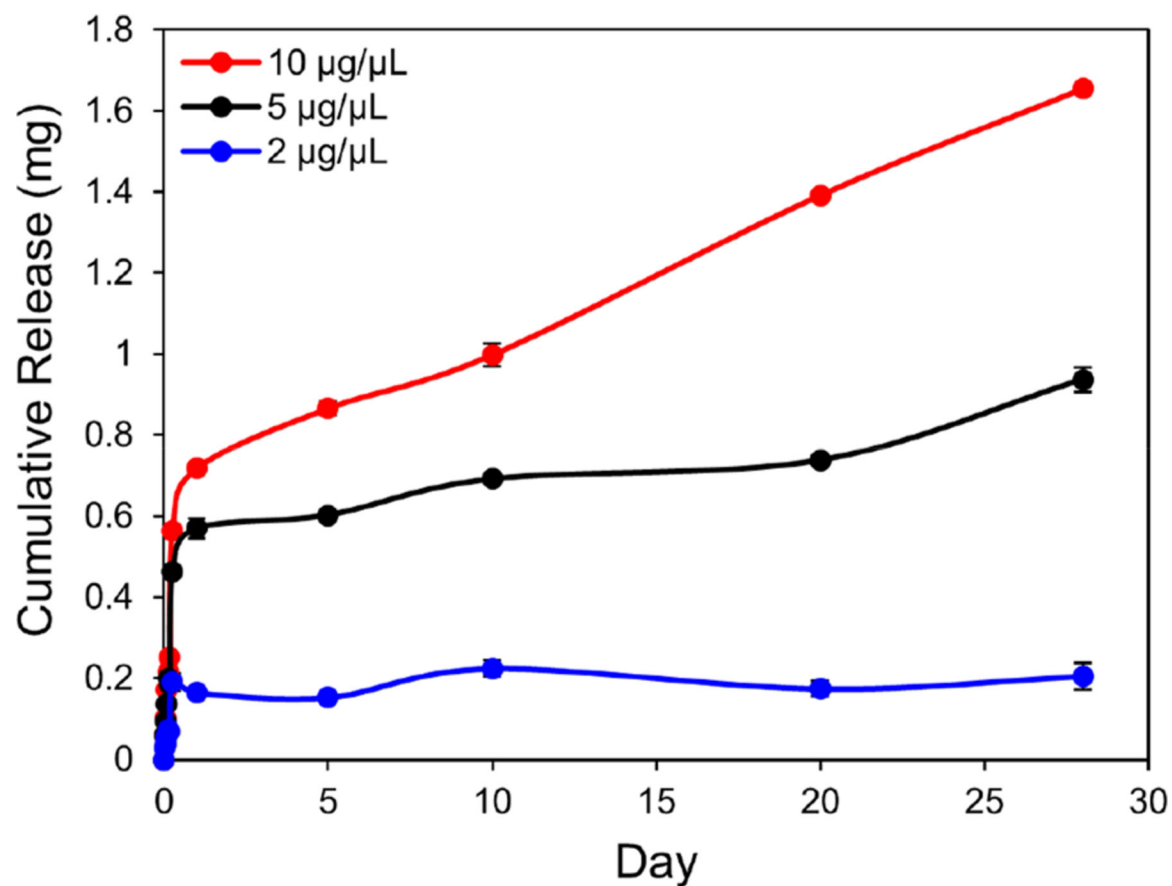
Figure 4.
Cumulative *in vitro* release of 4-AP from PLGA–PEG in PBS (pH 7.4) at 37 °C. PLGA–
PEG carriers exhibited an overall burst biphasic profile with a burst release of 4-AP within 1
day followed by release of a low maintenance dose for approximately 28 days. Cumulative
release was proportional to total loaded amount of 4-AP. Data are expressed as means ±
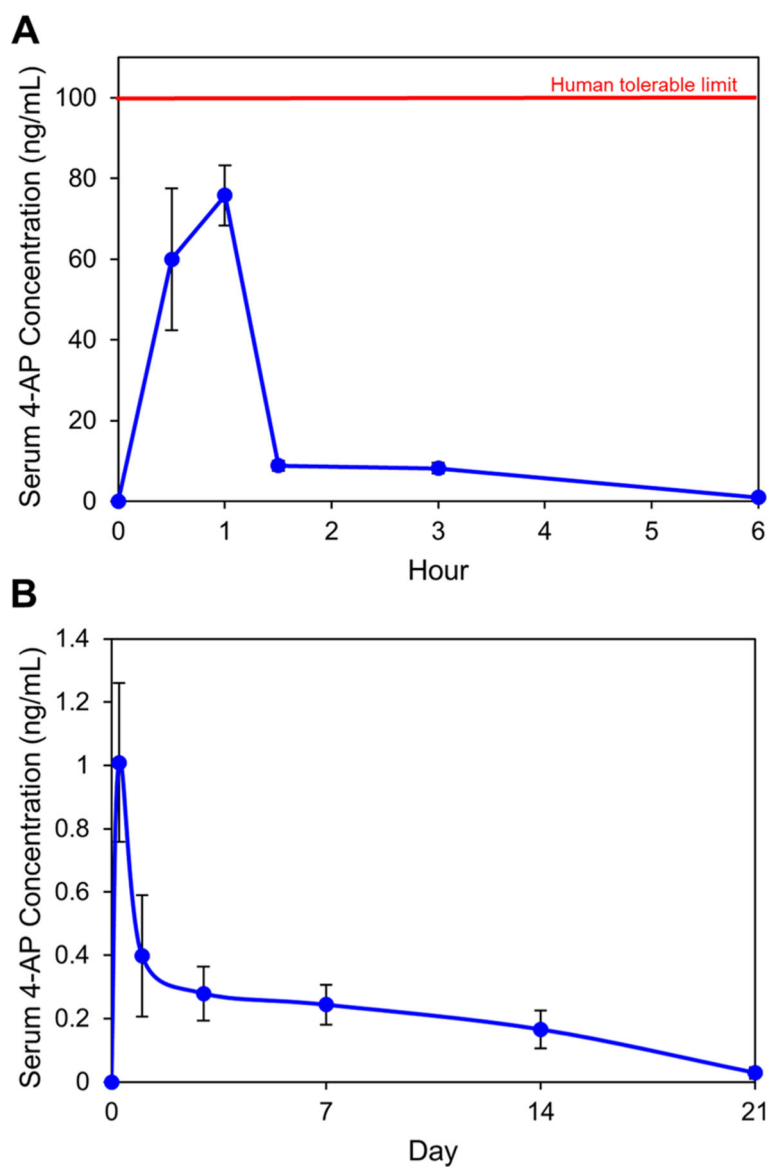SEM, $n = 3$/group.

Figure 5.
Pharmacokinetic study of 4-AP serum levels in mice after 2 μg/μL (4-AP)–PLGA–PEG administration at a 4-AP dose of 1.4 mg/kg. (A) 4-AP serum levels peaked 1 h after administration and never exceeded the human tolerable limit of 100 ng/mL. (B) 4-AP serum levels were nearly undetectable by Day 21. Data are expressed as means ± SEM, $n = 9$/group.
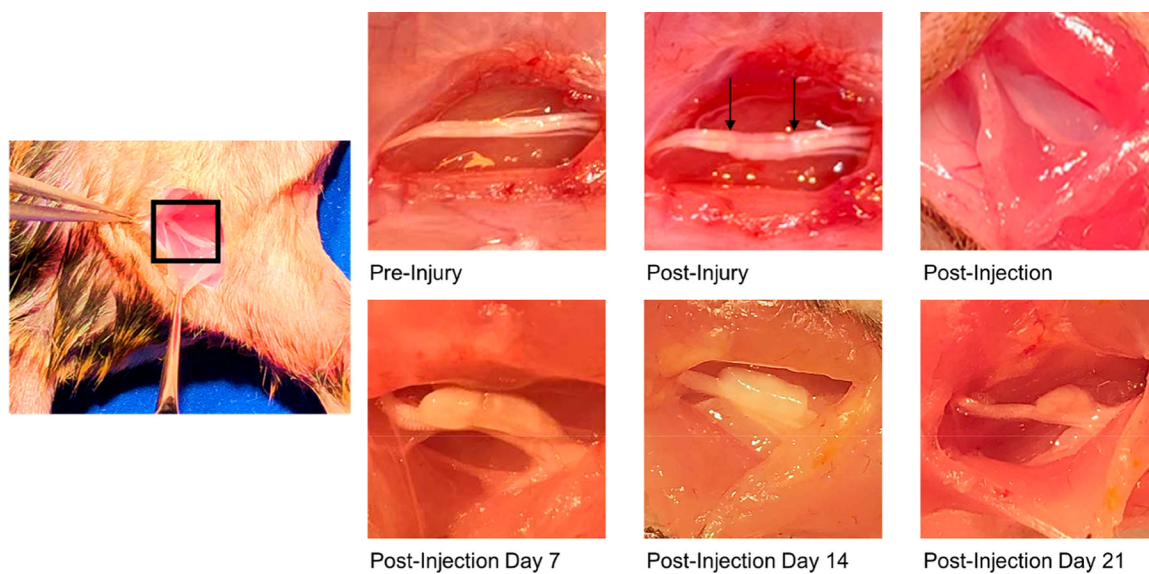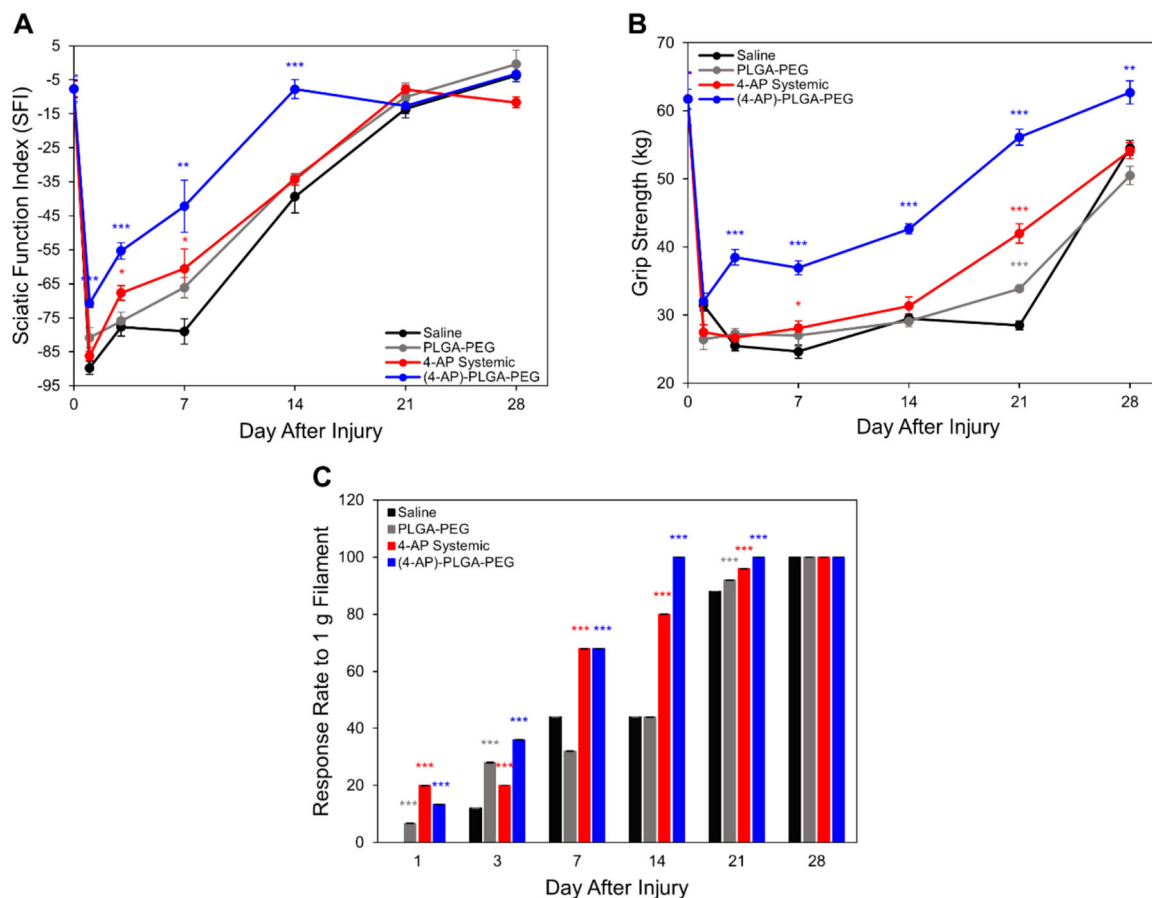
Figure 6.

In vivo biodegradation study of (4-AP)–PLGA–PEG. Pre-injury shows the mouse sciatic nerve. Post-injury shows the nerve after a moderate crush injury, as depicted by the arrows. Upon administration on the sciatic nerve post-injury, (4-AP)–PLGA–PEG turns opaque, indicating thermogelation. On post-injection days 7, 14, and 21, the gel remained directly on the nerve, although its mass decreased over time due to controlled polymeric degradation.

Figure 7.
Effects of (4-AP)–PLGA–PEG on motor and sensory functional outcomes. (A) (4-AP)–PLGA–PEG significantly improved SFI on post-injury days 1, 3, 7, and 14 compared to saline, PLGA–PEG, and systemic 4-AP groups. (B) (4-AP)–PLGA–PEG significantly improved grip strength on post-injury days 3, 7, 14, 21, and 28 compared to all other treatment groups. (C) (4-AP)–PLGA–PEG significantly improved withdrawal reflex (percent response to filament) as compared to the saline group on post-injury days 1, 3, 7, 14, and 21. Data are expressed as means ± SEM, $*p < 0.05$, $**p < 0.01$, and $***p < 0.001$ vs saline group, $n = 5$/group.
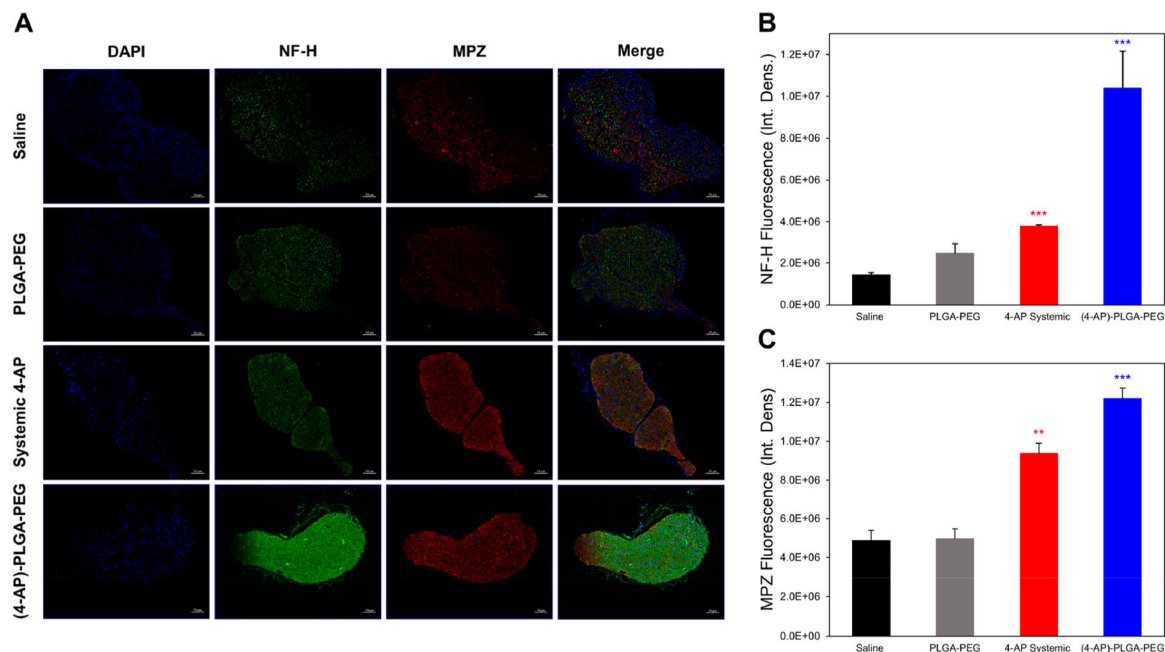
Figure 8.
Effects of (4-AP)–PLGA–PEG on immunohistochemical markers of nerve regeneration. (A) Representative transverse sciatic nerve immunofluorescent images of nuclei (DAPI), NF-H, and MPZ on post-injury day 28. Each image represents nine images from three different mice. Scale bar: 50 μm; magnification: 20×. (B) Quantification of NF-H integrated density on post-injury day 28. (4-AP)–PLGA–PEG-treated nerves contained significantly more NF-H protein in the lesion area than nerves from saline-treated animals. (C) Quantification of MPZ integrated density on post-injury day 28. (4-AP)–PLGA–PEG-treated nerves contained significantly more MPZ in the lesion area than nerves from saline-treated animals. Data are expressed as means ± SEM, ** $p < 0.01$ and *** $p < 0.001$ vs saline group, $n = 3$/group.
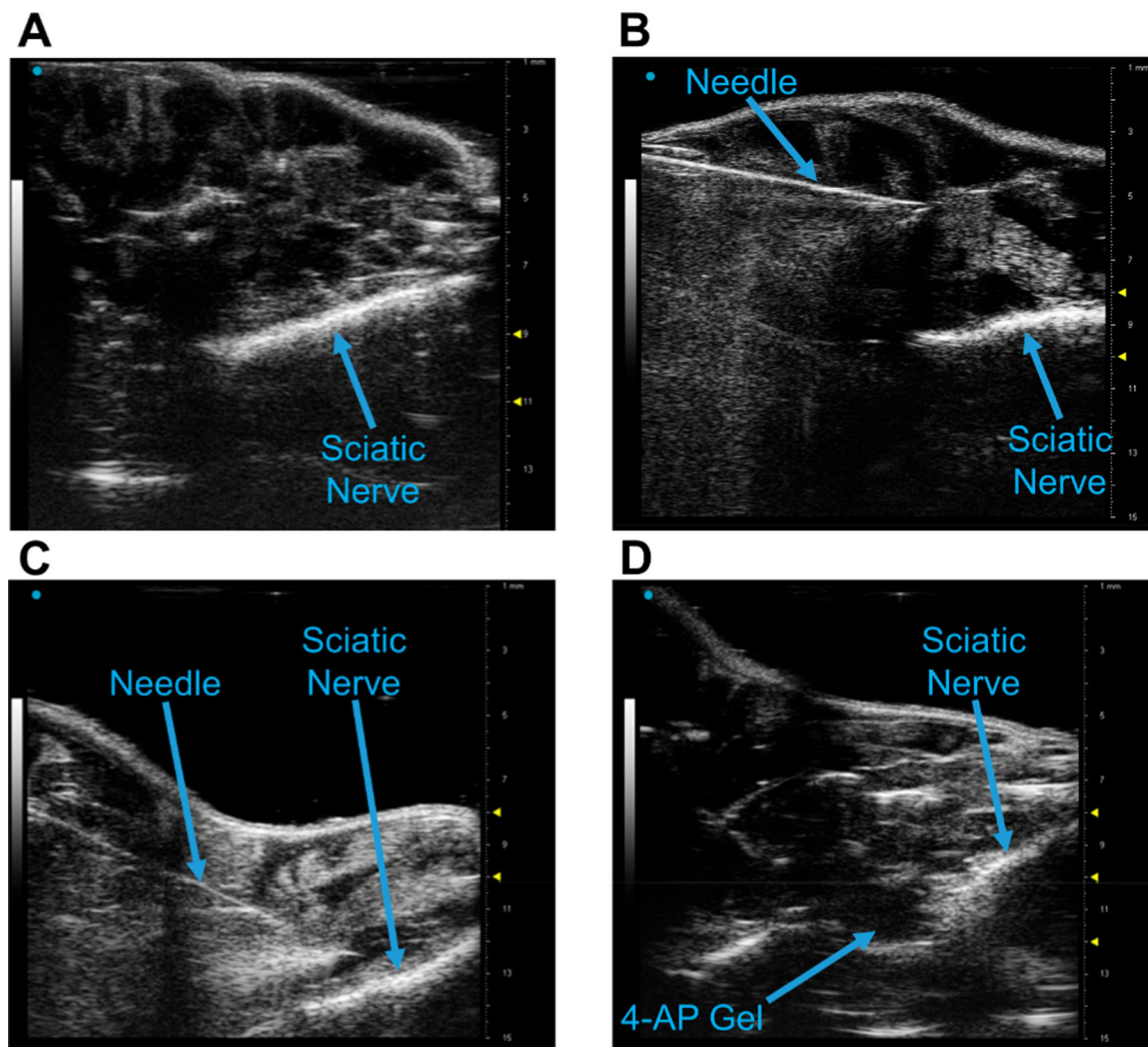
Figure 9.
(4-AP)–PLGA–PEG injection on the mouse sciatic nerve using small animal ultrasonography. (A) Longitudinal visualization of the sciatic nerve using the Vevo 3100 40 MHz ultrasound probe. (B) Identification of the 20 G needle with the nerve. (C) Positioning the needle over the sciatic nerve pre-injection. (D) Visualization of (4-AP)–PLGA–PEG on the sciatic nerve post-injection.